years ago. It is very likely that future progress in this area will be semiobservational and semitheoretical, with theory organizing a rich "zoo" of observed objects into a plausible evolutionary pattern.

References and Notes

1. H. A. Abt, *Annu. Rev. Astron. Astrophys.* **21**, 343 (1983).
2. V. Trimble, *Nature (London)* **303**, 137 (1983).
3. J. M. Retterer and I. R. King, *Astrophys. J.* **254**, 214 (1982).
4. J. V. Clausen, K. Gyldenkerne, B. Gronbech, *Astron. Astrophys.* **46**, 205 (1976).
5. D. M. Popper, *Astrophys. J.* **162**, 925 (1970).
6. ———, *Annu. Rev. Astron. Astrophys.* **18**, 115 (1980).
7. I. Iben, Jr., *ibid.* **12**, 215 (1974).
8. S. Chandrasekhar, *An Introduction to the Study of Stellar Structure* (Univ. of Chicago Press, Chicago, 1939); J. Liebert, *Annu. Rev. Astron. Astrophys.* **18**, 363 (1980).
9. R. N. Manchester and J. H. Taylor, *Pulsars*, (Freeman, San Francisco, 1977); W. Sieber and R. Wielebinski, Eds., International Astronomical Union Symposium No. 95, *Pulsars* (Reidel, Dordrecht, Netherlands, 1980).
10. J. N. Bahcall, *Annu. Rev. Astron. Astrophys.* **16**, 241 (1978).
11. P. C. Joss and S. A. Rappaport, *ibid.*, in press.
12. J. H. Taylor and J. M. Weisberg, *Astrophys. J.* **253**, 908 (1982).
13. S. L. Shapiro and S. A. Teukolsky, *Black Holes, White Dwarfs, and Neutron Stars* (Wiley, New York, 1983).
14. M. J. Rees, *Q. J. R. Astron. Soc.* **18**, 429 (1977); J. B. Hutchings, *Publ. Astron. Soc. Pac.* **95**, 799 (1983).
15. A. P. Cowley, D. Crampton, J. B. Hutchings, R. Remillard, J. Penfold, *Astrophys. J.* **272**, 118 (1983).
16. E. L. Robinson, *Annu. Rev. Astron. Astrophys.* **14**, 119 (1976).
17. J. S. Gallagher and S. Starrfield, *ibid.* **16**, 171 (1978).
18. J. Smak, *Acta Astron.* **17**, 255 (1967); J. Patterson, R. E. Nather, E. L. Robinson, F. Handler, *Astrophys. J.* **232**, 819 (1979).
19. J. E. Pringle, *Annu. Rev. Astron. Astrophys.* **19**, 137 (1981).
20. R. Hoshi, *Prog. Theor. Phys.* **61**, 1307 (1979); F. Meyer and E. Meyer-Hofmeister, *Astron. Astrophys.* **104**, L10 (1981); J. Smak, *Acta Astron.* **32**, 199 (1982); J. K. Cannizzo, P. Ghosh, J. C. Wheeler, *Astrophys. J.* **260**, L83 (1982); for a review, see J. Smak, *Publ. Astron. Soc. Pac.*, in press.
21. D. Sugimoto, D. Q. Lamb, N. D. Schramm, Eds., International Astronomical Union Symposium No. 93, *Fundamental Problems in the Theory of Stellar Evolution* (Reidel, Dordrecht, Netherlands, 1980).
22. B. Paczyński, paper presented at the First European Conference on Astronomy, Leicester, England, 1975 [reported by V. Trimble, *Q. J. R. Astron. Soc.* **17**, 31 (1976)].
23. E. W. Gottlieb, E. L. Wright, W. Liller, *Astrophys. J.* **195**, L33 (1975); E. B. Fomalont, B. J. Geldzahler, R. M. Hjellming, C. M. Wade, *ibid.* **275**, 802 (1983).
24. B. Margon, H. C. Ford, S. A. Grandi, R. P. Stone, *ibid.* **233**, L63 (1979); J. I. Katz, S. F. Anderson, B. Margon, S. A. Grandi, *ibid.* **260**, 780 (1982); K. Davidson and R. McCray, *ibid.* **241**, 1082 (1980).
25. H.-C. Thomas, *Annu. Rev. Astron. Astrophys.* **15**, 127 (1977).
26. F. H. Shu and S. H. Lubow, *ibid.* **19**, 277 (1981).
27. S. Refsdal, M. L. Roth, A. Weigert, *Astron. Astrophys.* **36**, 113 (1974).
28. J. P. Ostriker, personal communication; B. Paczyński, in International Astronomical Union Symposium No. 73 (Reidel, Dordrecht, Netherlands, 1976), p. 75; H. Ritter, *Mon. Not. R. Astron. Soc.* **175**, 279 (1976); R. E. Taam, P. Bodenheimer, J. P. Ostriker, *Astrophys. J.* **222**, 269 (1978); F. Meyer and E. Meyer-Hofmeister, *Astron. Astrophys.* **78**, 167 (1979); M. Livio, J. Saltzman, G. Shaviv, *Mon. Not. R. Astron. Soc.* **188**, 1 (1980); M. Livio, *Astron. Astrophys.* **105**, 37 (1982).
29. H. E. Bond, in *Cataclysmic Variables and Low-Mass X-Ray Binaries*, J. Patterson and D. Q. Lamb, Ed. (Reidel, Dordrecht, Netherlands, in press).

30. This work was supported by NSF grant AST-8317116.

Dynamic Structure of Membranes by Deuterium NMR

Rebecca L. Smith and Eric Oldfield

Summary. Progress in our understanding of the dynamic structure of membrane lipids and proteins has recently been made possible by the advent of high-field "solid-state" nuclear magnetic resonance spectroscopic studies of specifically deuterium-labeled systems. Major features of lipid and protein dynamics have been deduced.

Cell membranes are composed predominantly of lipids, proteins, and sterol molecules and are responsible for a wide variety of biochemical processes, including respiration, vision, photosynthesis, cell-cell recognition, and nerve impulse transmission. Not surprisingly, then, considerable efforts have been spent over the years in trying to characterize both the molecular structures of and intermolecular interactions between the individual membrane components in an attempt to relate the structure of membranes to their function. One of the most successful models of membrane structure which has emerged is the 1972 fluid mosaic model of Singer and Nicolson (*1*). This envisions membrane proteins as being dispersed in a fluid, liquid crystalline lipid bilayer, and is undoubtedly correct for many membrane systems. It is, however, by its nature a macroscopic rather than microscopic model of membrane structure, and there is now considerable interest in obtaining more detailed information on the actual structural details of, for example, protein-lipid interactions, or on the static and dynamic structure of membrane proteins (*2, 3*).

In this article we discuss recent advances in our understanding of lipid and protein dynamics in membranes, including some details of lipid-protein and lipid-sterol interactions and of cell surface dynamics, which have been made available primarily by observations of deuterium nuclear magnetic resonance (NMR) spectra of specifically ^{2}H-labeled species incorporated into both model and intact functional biological membranes. Such detailed experiments were not technically feasible at the time of the Singer-Nicolson hypothesis (*1*), when only relatively crude information on membrane structure could be obtained by the ^{2}H NMR method (*4, 5*). Recent advances in instrumentation—specifically the availability of high-field superconducting magnets for added sensitivity and improved pulse techniques for improved spectral line shape rendition (*6*)—now permit data acquisition at rates three or four orders of magnitude higher than in the early studies. This has opened up new vistas in membrane research, in particular, as discussed below, in the ability to monitor dynamic events in membrane proteins themselves.

Information from Spectra

Currently, most NMR studies of membrane structure employ the ^{2}H NMR method with high-field (~ 3.5 to 11.7 tesla) superconducting magnets and Fourier transform pulse methods (*6*) to investigate the line shapes, quadrupole splittings, and spin-lattice relaxation times of specifically ^{2}H-labeled species (lipids, sterols, or amino acids in proteins) introduced into the system of in-

Rebecca L. Smith is a research assistant and Eric Oldfield is a professor of chemistry at the University of Illinois at Urbana-Champaign, Urbana 61801.

terest. The theoretical background appropriate for consideration of the ^2H NMR spectra of lipid membranes has been discussed in some detail (*2, 3, 7–12*), so we shall be content to briefly quote the principal results. For the ^2H nucleus (with spin $I = 1$ and an asymmetry parameter $\eta = 0$ for the C–^2H bond) the allowed transitions correspond to $+1 \leftrightarrow 0$ and $0 \leftrightarrow -1$ and give rise to a quadrupole splitting of the NMR absorption line with a separation between peak maxima of

$$\Delta\nu_Q = \frac{3}{2}\frac{e^2qQ}{h}\frac{3\cos^2\theta - 1}{2} \qquad (1)$$

where e^2qQ/h is the deuterium quadrupole coupling constant, which has been found to be about 170 to 180 kHz for C–^2H bonds (*13*), and θ is the angle between the principal axis of the electric field gradient tensor at the deuterium nucleus and the magnetic field, H_0. For a rigid polycrystalline solid all values of θ are possible, and one obtains a so-called powder pattern line shape (Fig. 1A) in which the separation between peak maxima is about 130 kHz and the separation between the distribution steps is twice this value. In membranes, however, there is usually considerable motion of the C–^2H vector—due, for example, to methyl group rotation, *gauche-trans* isomerization in a hydrocarbon chain, or flipping of a benzene ring about its C_2 axis. It is thus generally necessary to take an average in time of $(3\cos^2\theta - 1)$ for the type of motion occurring (*14*). Not only does this cause a decrease in the overall breadth of the NMR line, but the shape may also be changed (*14–18*). Theoretical line shapes for a rigid aromatic residue, a methyl group rotating rapidly about its C_3 axis, and an aromatic residue undergoing twofold flips (in phenylalanine) are shown in Fig. 1, A to C.

Information on the actual rates of motion may also be deduced from line shape analysis (*11, 15–18*), at least in a sensitive window of correlation times ($\sim 10^3$ to 10^7 sec^{-1}) centered around $\sim 2 \times 10^5$ Hz (the rigid lattice quadrupole coupling constant); these and other faster (for instance, 10^7 to 10^{10} sec^{-1}) motions may also be investigated by using spin-lattice relaxation time (T_1) measurements (*9, 10, 19–21*), and slower motions may be investigated by T_2 and spin-alignment techniques (*22*). Figure 1D shows a typical T_1 determination for the methyl group of DL-[γ-$^2H_6$]valine crystals at room temperature. The magnetization of the sample is first inverted by means of a 180° radio-frequency pulse, and then the recovery of the magnetization is monitored by the quadrupole echo method, as shown in Fig. 1E (*6*). The recovery curve yields T_1, in this case 19.9 msec, corresponding to a correlation time, τ_c, of $\sim$ 140 psec (*20*). Thus, observation of ^2H NMR spectral line shapes and relaxation times in most instances provides information on both the rate and the type of motion undergone by a particular ^2H-labeled residue.

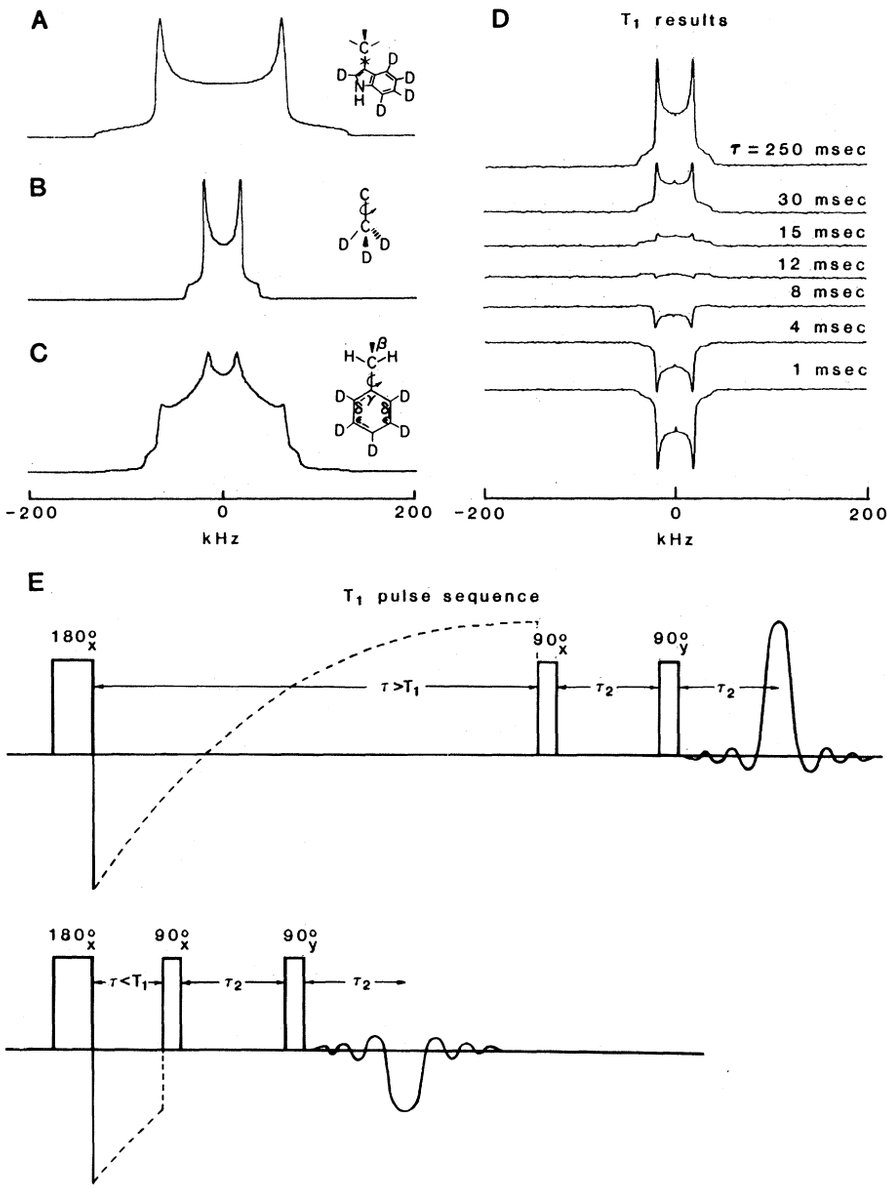

Fig. 1. Theoretical ^2H NMR powder patterns and line shapes. (A) Rigid aromatic residue. (B) Methyl group rotating about C_3 axis. (C) Phenyl group undergoing fast twofold "flip" about C^γ–C^ζ. (D) Partially relaxed deuterium inversion-recovery quadrupole echoes from polycrystalline DL-[γ-$^2H_6$]valine at 55.3 MHz; the τ values in the relaxation experiment are given in milliseconds. (E) Inversion recovery, quadrupole echo T_1 experiment; τ is a variable delay on the order of the T_1 and τ_2 is a fixed delay of 50 to 100 μsec.

Dynamics of Phospholipids and Glycolipids

Most of the lipids in biological membranes are known to undergo transitions from a thermotropic gel to a liquid crystalline phase (*23*), and ^2H NMR spectroscopy has been used with great success to investigate the organization of polar headgroups and backbone and hydrocarbon chain regions in phospholipids and glycolipids (*6, 24–26*).

In the polar regions of both phospholipids and glycolipids, it has been shown that the fatty acyl chain conformations are similar, including a bend at the 2 position of the *sn*-2 chain (*27, 28*). Also, each phospholipid headgroup has its own characteristic set of spectroscopic parameters which is not influenced significantly by the structure of the rest of the molecule—for instance, the presence of

hydrocarbon chain unsaturation. Furthermore, phosphatidylcholine (PC), phosphatidylethanolamine (PE), and phosphatidylglycerol (PG) headgroups have similar structures, while phosphatidylserine (PS) is more rigid, but all undergo very restricted motions (*24*). The PE and PC headgroups apparently lie flat, with their zwitterionic dipoles in the plane of the membrane (*24, 29*), at least in pure lipid bilayers, while with the glycolipid *N*-palmitoylgalactocerebroside (PGAC), the polar headgroup is essentially perpendicular to the membrane surface, projecting into the aqueous phase (*30*).

In the hydrocarbon chain region of liquid crystalline phospholipids and glycolipids, ^{2}H NMR results reveal a rather surprising general agreement between the spectra of different lipids labeled at a given site, when they are compared at the same reduced temperature. Results with intact biological membranes, such as those of *Escherichia coli* and *Acholeplasma laidlawii* B, are also virtually indentical to those of extracted lipids or of synthetic phospholipid multibilayers (*31–35*), and in almost all instances show little, if any, effect of membrane protein on lipid hydrocarbon chain structure. For example, spectra of 4-, 6-, 8-, and 14-^{2}H-labeled 1,2-dimyristoyl-*sn*-glycero-3-phosphocholine at ~ 23°C (just above the gel–liquid crystal phase transition temperature) are, within experimental error, the same as those of *A. laidlawii* B (PG9) grown in the presence of the corresponding tetradecanoic acids and avidin (which blocks endogenous fatty acid synthesis), and their extracted lipids, when examined at 46°C (just above the end of the gel–liquid crystal phase transition in the membrane) (*8, 32*). This clearly shows, at least in the *A. laidlawii* system, that protein does not have a significant effect on hydrocarbon chain order, and the actual structure of a chain will simply be a function of its reduced temperature. Several statistical mechanical models of hydrocarbon chain organization analyzing the ^{2}H NMR results have been described (*36, 37*). One important result is the ability to determine lipid bilayer membrane thicknesses (*37*), the values obtained being in excellent agreement with those determined directly by neutron diffraction methods (*8, 29*).

Below T_c, lipids form a variety of crystalline or gel phases, generally characterized by a sharp 4.1 Å^{-1} Bragg reflection in x-ray diffraction experiments. Recent advances in NMR instrumentation now permit more detailed analysis of the dynamic structures of such phases, and results on PC, PE, and cerebroside have been reported (*15–17*), together with preliminary results on gel state lipid in the *A. laidlawii* membrane system (*5, 35*).

The results for the liquid crystalline phase of cerebroside are virtually indistinguishable from those obtained with phospholipids at the same reduced temperature (*28*). However, in the crystalline phase of *N*-palmitoylgalactocerebroside, which occurs below about 82°C (*28, 38*), ^{2}H NMR line shapes corresponding to a rather unusual asymmetry parameter ($\eta = 1$) are obtained, as shown in Fig. 2. These line shapes appear to originate from nonzero asymmetry parameters due to "hopping" between two (or more) sites (*15*) in the crystalline phase. Such motions are not uncommon in NMR spectroscopy of, for example, salt hydrates, where water molecules flip about their HOH bisector at very rapid rates (*14, 39*). Typical spectra for high-temperature crystalline gel cerebroside ($\eta = 1.0$, 55°C) are compared with spectra for the more normal crystalline gel ($\eta = 0$, −40°C) and the liquid crystalline phase ($\eta = 0$, 85°C) in Fig. 2. The "triangular" line shape seen at 55°C is characteristic of rapid movement of the C-^{2}H vector from one site to another across the tetrahedral angle (*14, 15*), due to *gauche-trans* isomerization (Fig. 2C). In the limit of fast exchange, and assuming equal populations of the two isomers, the expected spectrum is easily calculated (*14, 15*). The component along Z is unaffected by the motion and is $\omega_\perp$, while the component along Y is zero since the two C-^{2}H vectors are, by virtue of the tetrahedral bonding, at the "magic angle" with respect to this direction. Since the tensor must be traceless, the third (X) component is $-\omega_\perp$. With this type of twofold motion between equally populated sites and with $e^2qQ/h \sim 170$ kHz, the spectrum is axially asymmetric ($\eta = 1$) and its breadth is ~ 120 kHz. At lower temperatures, the rates of motion and the number of *gauche* conformers in the chain decrease, and more complex line shape analyses are required to interpret the results shown in Fig. 2B. Nevertheless, both the jump rate and the *gauche* probabilities may be determined (*15*).

Although there have been few reports of low-temperature (gel phase) spectra of intact biological membranes (*5, 35*), the broad line shapes that have been observed may also originate in similar two-site *gauche-trans* hopping, as demonstrated in the case of galactocerebroside. The significance of crystalline-state lipids in some intact biological membranes in which only restricted rotational isomerization occurs remains one of the more puzzling features of the mosaic structure of cell membranes. Indeed, there are

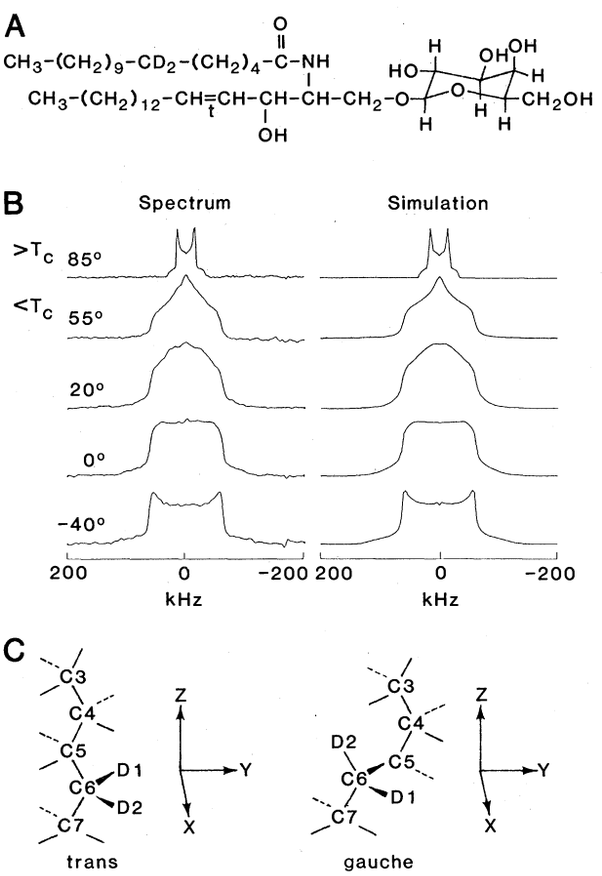

Fig. 2. (A) Structure of *N*-palmitoylgalactosylceramide (PGAC). (B) (Left) Experimental 45.2-MHz ^{2}H NMR spectra of aqueous dispersions of 6,6-d_2PGAC, 50 percent H_2O by weight, obtained as a function of temperature. (Right) Theoretical simulations of the experimental spectra. The following parameters were used: at −40°C, population probability ratio $P_1:P_2 = 0.98:0.02$; jump rate $k_{12} = 3 (\pm 2) \times 10^3$ sec^{-1}; at 0°C, $P_1:P_2 = 0.8:0.2$, $k_{12} = 2.5 (\pm 0.5) \times 10^5$ sec^{-1}; at 20°C, $P_1:P_2 = 0.7:0.3$, $k_{12} = 9 (\pm 2) \times 10^5$ sec^{-1}; at 55°C, $P_1:P_2 = 0.5:0.5$, $k_{12} \geq 3 \times 10^6$ sec^{-1}; and at 85°C, axially symmetric spectrum with $\Delta\nu_{Q_\perp} = 28.2$ kHz. Uncertainties in P_1 and P_2 are 5 to 10 percent. (C) Twofold jump isomerization in a polymethylene chain segment from *trans* to *gauche*. Note that in the *gauche* configuration D1 assumes the orientation originally occupied by D2.

reasons to believe that, at least in mammalian cells, the presence of gel-state lipid may cause improper cell function (*40*), but that this situation may be ameliorated by the presence of cholesterol (*40, 41*), as discussed below.

Cholesterol in Membranes

Cholesterol is a rigid tetracyclic sterol having the following structure:

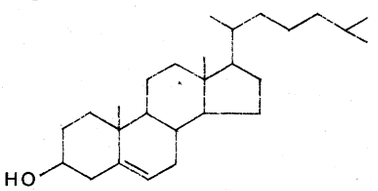

Despite its wide occurrence in biological membranes, there have been relatively few studies aimed at determining its static and dynamic organization in the bilayer. Early ^{13}C NMR studies of model membranes by Opella *et al.* (*42*) indicated that the isopropyl section of the side chain had considerable rotational freedom, while the sterol ring itself underwent highly anisotropic motion. Similar results have also been obtained with ^{2}H NMR. In particular, it appears that the sterol molecule undergoes rapid axial diffusion (greater than 10^{7} sec^{-1}), together with a slight off-axis "wobble" motion, which is a function of temperature and lipid bilayer composition (*8, 43, 44*). The correlation time for the motion about the long axis has been accurately determined by ^{2}H NMR T_1 measurements on [7-^{2}H]cholesterol in a PG bilayer, where observation of a T_1 minimum yields a correlation time of 3.5×10^{-9} sec rad^{-1} (*45*). Typical values of off-axis fluctuations are around 10° to 15° (*8*). In addition, the results of recent ^{2}H NMR studies indicate that the C-8 side chain appears essentially rigid out to C_{23} (*45*). This rigidity, in combination with the rigid all-*trans* nature of the tetracyclic sterol nucleus and the lack of any large side chains protruding from the sterol α and β surfaces, causes the cholesterol molecule to act as a rigid wall in lipid bilayer structures, resulting in a condensing or ordering effect, which has been investigated extensively by ^{2}H NMR (*4, 8, 43–49*). Above T_c, the cholesterol molecule orders the hydrocarbon chains of fluid lipid bilayers [in addition, it is thought, to acting as a "spacer" for the polar headgroup region (*8*)]. Below T_c, however, cholesterol prevents lipid hydrocarbon chains from crystallizing into the more ordered crystalline or gel phases, in the case of both phospholipids and cerebrosides (*28*). Above T_c, changes in hydrocarbon chain length on addition of cholesterol have been deduced from the NMR data, and the results compare well with those obtained by neutron diffraction (*8*). For example, a bilayer thickness of about 31 Å [at the level of the C-2 chain segment in a dimyristoylphosphatidylcholine (DMPC)–30 mole percent cholesterol bilayer] is calculated from the NMR results, which compares favorably with the value of 33 Å obtained from neutron diffraction results (*8*). Deuterium NMR spectra showing the large effects of cholesterol in intact biological membranes, in particular in the *A. laidlawii* B system, have also been reported (*47*), again corresponding to an increase in effective thickness of the lipid hydrocarbon chain region.

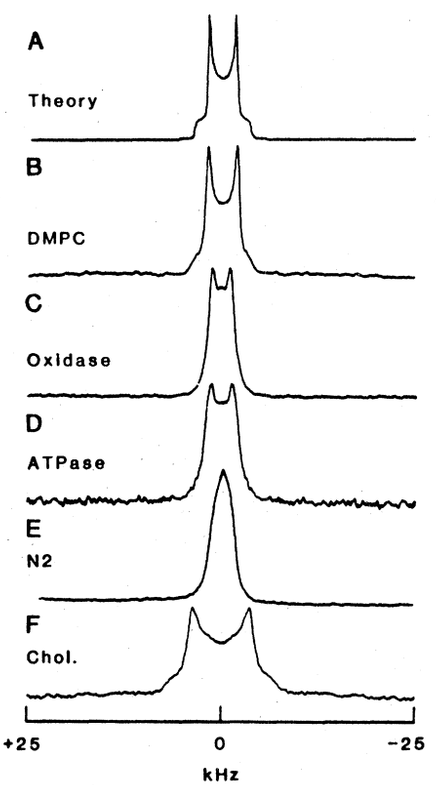

Fig. 3. Theoretical and experimental ^{2}H NMR spectra of ^{2}H-labeled lipids, showing the effects of proteins and cholesterol on hydrocarbon chain order. (A) Theoretical ^{2}H powder pattern; the splitting is arbitrary. (B) l-Myristoyl-2(14,14,14-trideutero)myristoyl-*sn*-glycero-3-phosphocholine (DMPC-d_3) in excess water at 30°C. (C) As in (B), but lipid contains 67 percent by weight cytochrome *c* oxidase (E.C. 1.9.3.1). (D) As in (B), but lipid contains 67 percent by weight sarcoplasmic reticulum adenosinetriphosphatase (E.C. 3.6.1.3). (E) As in (B), but lipid contains 67 percent by weight beef brain myelin proteolipid apoprotein (N2). (F) As in (B), but lipid contains 33 percent by weight cholesterol. Deuterium NMR spectra were obtained by the quadrupole-echo Fourier transform method at 5.2 T (corresponding to a deuterium resonance frequency of 34 MHz).

Effects of Proteins on Lipid Dynamics

The nature of protein-lipid interaction in biological membranes and in reconstituted lipid-protein systems is of considerable interest from a biochemical standpoint (*50, 51*), but the subject has unfortunately been plagued by considerable controversy over the past 10 years. An early version of protein-lipid interaction in biological membranes (*52*) suggested, at least at high protein-lipid ratios, that lipid molecules were "immobilized" on the surface of several membrane proteins, and lipid titration and integrated-intensity experiments indicated that only the first layer of lipid adjacent to protein was strongly immobilized in this way. This led to the idea of a boundary lipid or annulus (*53*) of highly ordered lipid adjacent to membrane proteins, which several theoreticians then modeled as rigid rods or hexagonal cylinders of protein molecules penetrating the lipid bilayer, in much the same way as cholesterol, thereby prohibiting the normal flexing of the lipid hydrocarbon chains characteristic of liquid crystalline phospholipids. While proteins may have complex effects on collective modes in lipid bilayers, ^{2}H NMR studies of similar systems (*54–62*) have given no evidence for ordering of lipid hydrocarbon chains by a variety of proteins. The observed ^{2}H NMR spectra of protein-lipid recombinants in almost all instances are virtually identical to those of the pure lipid bilayers, in accord with observations on intact cell membranes (*31–35*), whereas those of lipid-cholesterol systems typically have an approximately twofold increase in quadrupole splitting; that is, the lipid hydrocarbon chains in lipid-cholesterol systems are approximately twice as ordered as those in a pure lipid bilayer, or protein-lipid (2:1 by weight) complex, as shown in Fig. 3. This has naturally led to the development of models in which there are, in general, no strong lipid-protein interactions in membranes. In addition, the ^{2}H NMR results [and, more recently, electron spin resonance (ESR) results (*59, 60, 62*)] indicate that in many systems there is probably rapid exchange between free bilayer lipid and lipid adjacent to the protein surface (*51, 55–62*), and that the conformation of lipid hydrocarbon chains adjacent to the protein surface is probably only slightly different from that in a pure lipid bilayer.

The question thus arises of the reason for the apparent disagreement between early results, based on ESR spin-labeling experiments, indicating a rigid boundary-layer annulus of lipid surrounding and presumably controlling the enzymat-

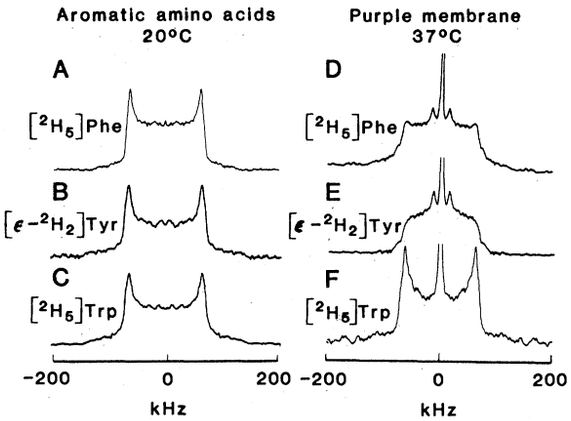

Fig. 4. Deuterium NMR spectra of polycrystalline aromatic amino acids at 20°C and of aromatic amino acids incorporated into the purple membrane of *H. halobium* at 37°C. (A) [$\delta_1,\delta_2,\epsilon_1,\epsilon_2,\zeta$-$^2H_5$]Phenylalanine, (B) [$\epsilon_1,\epsilon_2$,-$^2H_2$]tyrosine, (C) [$\delta_1,\epsilon_3,\zeta_2,\zeta_3,\eta_2$-$^2H_5$]-tryptophan, (D) [$\delta_1,\delta_2,\epsilon_1,\epsilon_2,\zeta$-$^2H_5$]phenylalanine-labeled purple membrane, (E) [ϵ_1,ϵ_2-$^2H_2$]tyrosine-labeled purple membrane, (F) [$\delta_1,\epsilon_3,\zeta_2,\zeta_2,\eta_2$-$^2H_5$]tryptophan-labeled purple membrane.

ic activity of a membrane protein, and more recent ^2H NMR (and ESR) results, showing the dynamic nature of the interaction. One possibility is that the ESR labels undergo some type of specific interaction with the protein surface—for instance, hydrogen bonding from the polar isoxazolidine ring to the peptide backbone (*63*). However, recent studies appear to rule out this explanation (*64, 65*), in which case it appears that the alternative "time scale" argument is applicable (*56, 57*). The explanation for the apparent discrepancy between NMR and ESR results probably originates in the different time scales applicable for conventional NMR ($\approx 10^{-5}$ sec) and ESR ($\approx 10^{-8}$ sec) experiments. Thus, a motion fast on the NMR time scale may be slow on the ESR time scale and may not substantially affect the ESR spectrum. It is thought by several workers (*59, 60, 66*) that the actual intermediate-rate motions involved correspond to lipid exchange on and off protein surfaces at rates of $\sim 10^6$ to 10^7 sec^{-1}, a result based on ESR spin-lattice relaxation times (*60*) and spectral simulations of spin-label data (*66*). The alternative explanation of intermediate-rate reorientation of lipid chains on the protein surface cannot, however, be ruled out (*59*). More quantitative NMR experiments are clearly needed in this area.

Below the temperature of the gel–liquid crystal phase transition of the pure lipid, protein has the effect of preventing lipid hydrocarbon chains from crystallizing into gel-state lipid (*55, 57*); however, the hydrocarbon chains are not "ordered" as they are with cholesterol at low temperatures (*46, 57*), due again, we believe, to the "rough" nature of protein surfaces. Overall, then, a general picture of protein-lipid interaction has arisen in which, at least above T_c, there are in general no long-lived regions of specific types of lipid molecules surrounding most membrane proteins. Rather, lipid molecules are in a highly fluid, dynamic state, colliding with the rough or irregular protein surfaces at high ($\sim 10^6$ to 10^7 sec^{-1}) rates. This is much faster than a typical enzyme turnover, so that for most systems it seems that "average" lipid properties should influence enzyme activity. Of course, exceptions to this general rule may be found, and we have observed apparently strong interactions between cardiolipin and cytochrome oxidase by ^{31}P NMR (*67*). There is no evidence, however, for any general ordering of the lipid hydrocarbon chains in protein-lipid "collision complexes," in contrast to the large effects seen with cholesterol-lipid interactions, as discussed above.

We should add, however, that such apparently good agreement between the NMR and ESR results is not strictly proven, and that other spectroscopic techniques, such as fluorescence polarization anisotropy (*68, 69*), suggest that protein molecules cause a tilting and ordering of lipid hydrocarbon chains. A plausible physical mechanism has not been provided, and further analysis of the fidelity of fully conjugated polyene species in reflecting processes such as *gauche-trans* isomerization remains to be performed.

Direct Observation of Side Chain Mobility in Proteins

Arguably the most significant systems to investigate in biological membranes are the membrane proteins themselves. Unfortunately, however, they are in general the most difficult to study spectroscopically because of their dilution. One exception is bacteriorhodopsin, the sole protein in the photosynthetic purple membrane of the obligate halophile *Halobacterium halobium* (*70*). In this section we discuss recent results for this system, together with results of studies on amino acid crystals, aimed at determining the rates and types of motion of individual types of amino acid side chains in a membrane protein. While similar studies have been carried out for proteins in solution by ^1H and ^{13}C NMR (*71*) and for crystals of soluble proteins (*72, 73*) by x-ray methods, it appears that the ^2H NMR method offers particular promise for investigating the dynamics of proteins in condensed phases, such as membranes or collagen (*3, 16, 18, 74, 75*), where high-resolution x-ray or solution NMR studies are not yet feasible. The ability to directly observe protein dynamics in intact membrane systems should make it possible to study the influence of lipid and sterol molecules on protein function.

Observation of [$^2H_3$]methyl-labeled amino acids such as alanine, threonine, valine, leucine, and methionine, in the crystalline solid state, yields information about the rates and types of side chain motion, which may be compared with those seen in intact biological membranes. However, in many cases it is found that only "rigid-lattice" spectra, characteristic of rapid C_3 rotation, are obtained, so that T_1 measurements are required to determine the rotational correlation times, τ_c. The T_1 values so determined may be interpreted in terms of a suitable mathematical model for relaxation (*19–21, 76*). When such determinations are made as a function of temperature, interesting information on the activation energies for motion is obtained. The results obtained to date suggest that the dynamics of methyl residues in membrane proteins are dominated by short-range interactions; and, indeed, experimental observations on bacteriorhodopsin containing biosynthetically incorporated [γ-$^2H_3$]threonine, [γ-$^2H_6$]valine, and [δ-$^2H_3$]leucine (*20*), at temperatures close to or below the growth temperature, reveal rates, types, and activation energies for motion that are very similar to those obtained with the amino acid crystals. Similar results are obtained with Thr-, Val-, and Leu-labeled *E. coli* cell membranes (*20*) enriched with either oleic or elaidic acid, the activation energies and τ_c values observed in the membrane protein being remarkably similar to those found for a variety of soluble proteins in solution (*20, 71*).

In the relatively long methyl-containing amino acid side chains, such as leucine and methionine, additional modes of motion appear to occur readily, causing changes in NMR line shapes and, in some instances, deviations from linearity in the Arrhenius curves. For example, in the case of [δ-$^2H_3$]leucine-labeled bacte-

riorhodopsin [and collagen (*74, 75*)], ^2H NMR line shapes having asymmetry parameters $\eta \rightarrow 1$ and reduced overall spectral breadths are obtained at $\sim 30°$ to 40°C. These results strongly suggest that the leucine side chain undergoes rapid ($\approx 10^6$ rad sec^{-1}) twofold jumps about C^{γ}–C^{δ} (*20, 74, 75*). The two conformers are presumably those observed in a variety of small peptide x-ray crystal structures (*77, 78*). In general, it is likely that as the length of a nonpolar side chain increases, the rates and types of side chain motion will increase. This idea is borne out by the observation (*20*) of spectra characteristic of multiple (three or four) site hopping in crystalline L-[ϵ-$^2H_3$]methionine (*20*). These complex motions are also likely to occur when such amino acids are incorporated into membrane proteins.

With the aromatic amino acids histidine, phenylalanine, tyrosine, and tryptophan, motions in membrane proteins are likely to be less complex than with the long-chain amino acids. Results have been obtained for a variety of ^2H-labeled tyrosines, phenylalanines, and tryptophans incorporated into bacteriorhodopsin and *E. coli* membranes (*3, 16, 18, 20*). Figure 4 shows typical spectra of [$^2H_5$]phenylalanine, [ϵ-$^2H_2$]tyrosine, and [$^2H_5$]tryptophan, incorporated into bac-

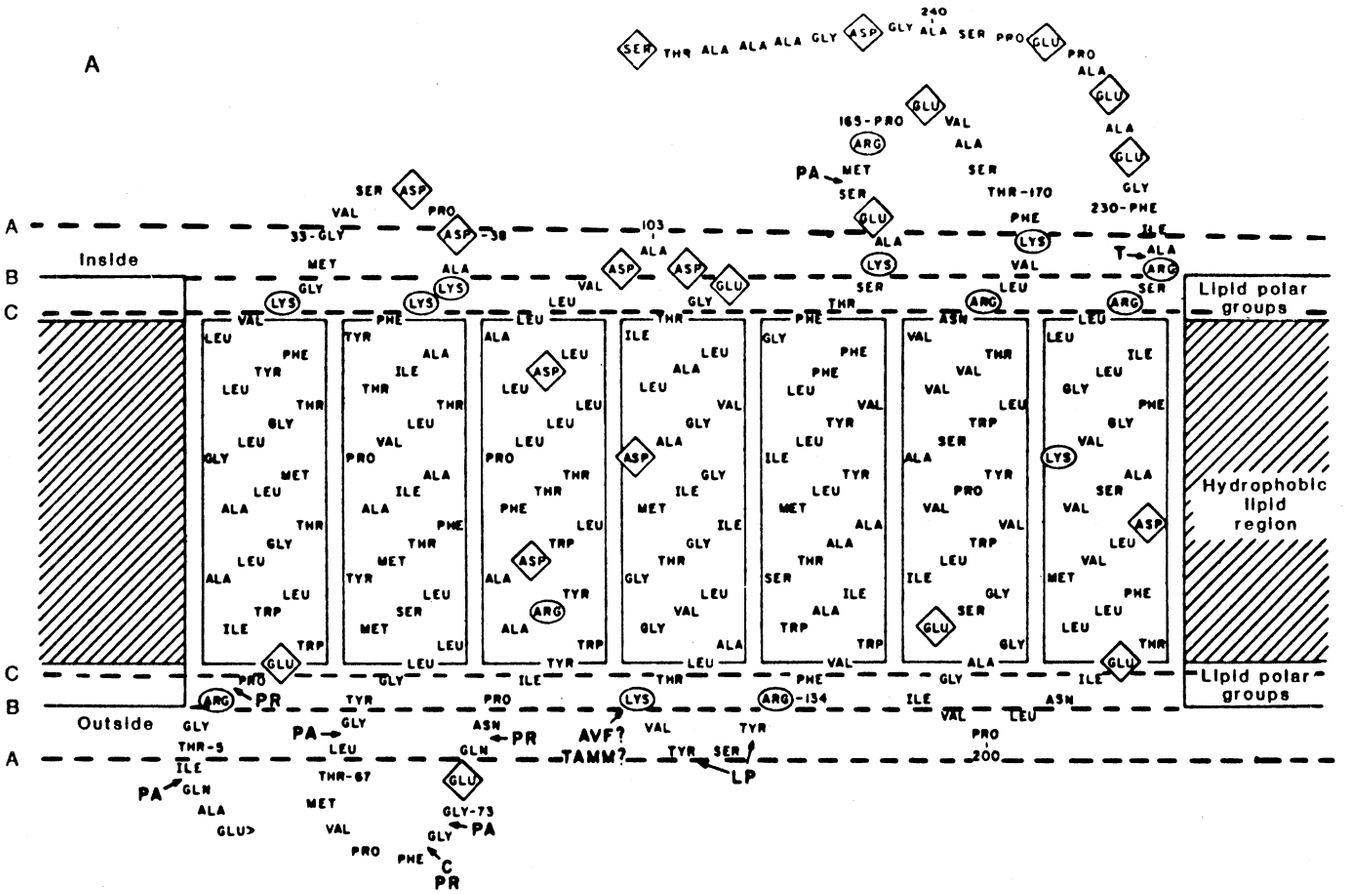

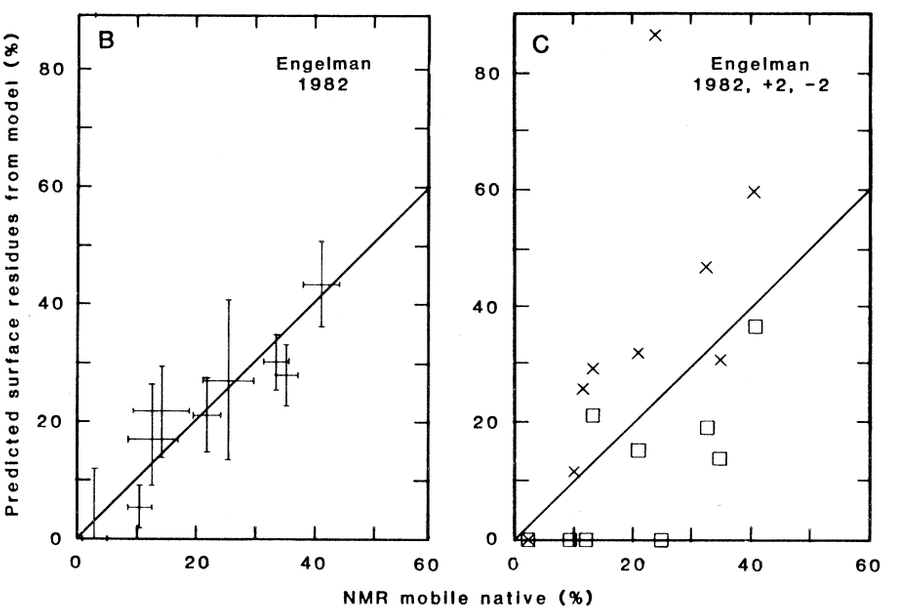

Fig. 5. Demonstration of mobility of surface residues in purple membranes. (A) Model of Engelman *et al.* (*82*), showing various definitions of the membrane surface. (B) Graph showing correlation between the percentage of residues above the membrane surface (B–B′) and the percentage of residues undergoing isotropic motion from the ^2H NMR experiment. (C) As in (B), but with two alternative definitions of the membrane surface: (□) A–A′ and (×) C–C′ in (A).

teriorhodopsin of the purple membrane of *H. halobium*, together with spectra of the free amino acids in the crystalline solid state.

Results with crystalline phenylalanine are quite complex (*3, 16, 76, 79*), and indicate that lattice forces have a dominant effect on side chain motion. For example, at room temperature the aromatic rings of phenylalanine hydrochloride are all relatively rigid (Fig. 4A). At the same temperature, free-base phenylalanine spectra display two components, corresponding to rigid ($\tau \sim 10^{-5}$ sec) and mobile ($\tau \sim 10^{-8}$ sec) rings. Because of the large differential spin-lattice relaxation times involved (~ 10 sec versus ~ 100 msec), it is possible to eliminate the rigid component by rapid pulsing, resulting in the production of a spectrum with an asymmetry parameter $\eta \sim 0.6$ (Fig. 1C) (*3, 16, 76, 79*). By contrast, spectra of ring-labeled tyrosine and tryptophan exhibit only a single, rigid-lattice component (Fig. 4, B and C).

Similar experiments with ^{2}H-labeled bacteriorhodopsin were performed recently (*3, 16, 76, 80, 81*). The results indicate that tryptophan, because of its large bulk, is relatively rigid at all temperatures (up to ~ 90°C, when the protein denatures). Spin-lattice relaxation times are ~ 20 sec at the temperature of growth, and relaxation is probably dominated by torsional oscillations.

At about −30°C, ^{2}H NMR spectra of tyrosine and phenylalanine in bacteriorhodopsin suggest that all such residues are also quite rigid, but as the growth

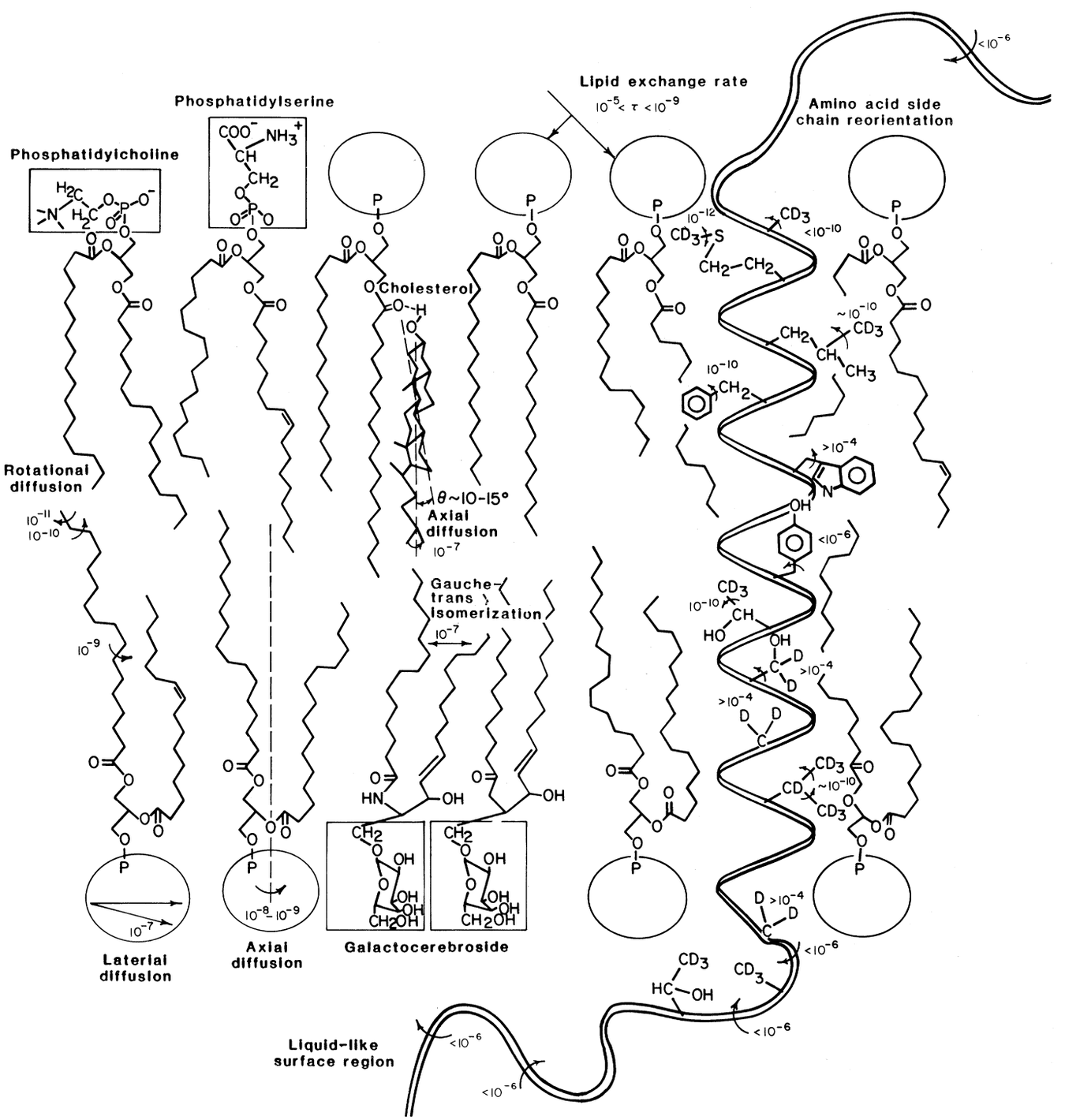

Fig. 6. Microscopic, dynamic model of a biological membrane. Correlation times are given in seconds.

temperature of 37°C is approached, most phenylalanine and tyrosine residues in the purple membrane become mobile, executing twofold flips about C^{β}–C^{γ} at rates of $\sim 10^6$ to 10^7 sec^{-1}. The type of motion may be deduced from the asymmetric line shape observed (Fig. 4, D and E). The observed asymmetry parameter of $\eta \sim 0.6$ is expected for a twofold jump over a 120° angle (*3, 14*) (Fig. 1C).

Protein Dynamics at a Membrane Surface

Determination of the rates and types of motion of amino acid residues at the membrane surface should be particularly interesting, since many receptors, antigens, and so forth are located in this region. Recently, there has been considerable progress in using the NMR method to probe membrane surface structure and the problem of membrane-membrane contact (*82*). We will give a brief account of this work and illustrate the potential for further studies.

As may be seen from Fig. 4, D to F, each of the ^2H NMR spectra of labeled purple membranes contains a sharp central component. Results of intensity measurements on samples extensively exchanged with deuterium-depleted water indicate that the central components of the spectra of all ^2H-labeled membranes arise primarily from highly mobile surface protein segments (*82*).

Figure 5A shows the polypeptide chain folding pattern for bacteriorhodopsin suggested by Engelman *et al.* (*83*), where we define a membrane surface (B–B′) together with a surface that is two residues farther outside (A–A′) or farther in (C–C′). If it is assumed that all residues outside the membrane surface are mobile, and thus give rise to a sharp, isotropic line, while all residues inside the surface are rigid or crystalline (on the ^2H NMR time scale), we obtain excellent agreement between the molecular model B–B′) and ^2H NMR intensity results with the following ^2H-labeled membranes: Gly, Val, Leu, Ileu, Ser, Thr, Lys, Phe, Tyr, Trp, and Arg (*82*) (Fig. 5B). Similar good agreement is obtained with the models of Ovchinnikov (*84*) and Khorana and co-workers (*85*), but the fit is noticeably worse with Engelman's earlier model (*82, 86*). Poor agreement is also obtained if the membrane surface is chosen one or two residues different from that shown (Fig. 5, A and C). Taken together, these results strongly suggest that (i) all surface residues in bacteriorhodopsin are highly mobile on the time scale of the ^2H NMR experiment, (ii) all amino acids in the membrane matrix are essentially crystalline, (iii) a membrane surface (± one residue) may be readily defined by NMR in bacteriorhodopsin, and (iv) the NMR results may be used to evaluate the various structural models proposed.

Microscopic Fluid Mosaic Model

As stated in the introduction, the past decade has witnessed an enormous increase in interest in applying ^2H NMR to analyze the microscopic structure of biological and model membranes. In the spirit of previous membrane model-builders and artists, we therefore outline in Fig. 6 a contemporary picture of membrane structure, illustrating the numerous new quantitative, dynamic features of membrane structure that have been deduced by ^2H NMR and other spectroscopic techniques.

The results presented in this article support the idea of a fluid mosaic model in which, in general, proteins are influenced only by the average properties of the fluid lipid bilayer—that is, the activities of membrane enzymes are not dominated by a special layer of boundary or annular lipid. Moreover, the great similarity between the (average) dynamic structures of amino acid side chains in crystals, in bacteriorhodopsin, in *E. coli* membranes, and in several proteins in solution suggests lack of a large general effect of protein environment on side chain dynamics. Lipid-mediated effects thus presumably occur at the level of molecular rotation and translation, or must involve specific interactions that are beyond current detection limits. Most likely, both types of effects are to be found.

In conclusion, we believe it is now apparent that NMR spectroscopy, in particular of the ^2H nucleus in isotopically labeled cells, can provide information on the rates and types of motion of essentially any type of grouping in a cell membrane. With even higher magnetic field strengths (for improved sensitivity) and methods for resolving individual residues—for instance, through genetic manipulation, reconstitution techniques, magnetic alignment to form ordered arrays, or crystallization of suitable systems—it should soon be possible to study the dynamic structure of an even wider variety of cell membrane components in short periods of time. Such NMR determinations are of the greatest interest, as such studies do not appear to be accessible by any other spectroscopic technique.

References and Notes

1. S. J. Singer and G. L. Nicolson, *Science* **175**, 720 (1972).
2. E. Oldfield *et al.*, *Biochem. Soc. Symp.* **46**, 155 (1981).
3. R. A. Kinsey, A. Kintanar, E. Oldfield, *J. Biol. Chem.* **256**, 9028 (1981).
4. E. Oldfield, D. Chapman, W. Derbyshire, *FEBS Lett.* **16**, 102 (1971).
5. ———, *Chem. Phys. Lipids* **9**, 69 (1972).
6. J. H. Davis, K. R. Jeffrey, M. Bloom, M. I. Valic, T. P. Higgs, *Chem. Phys. Lett.* **42**, 390 (1976).
7. J. Seelig, *Q. Rev. Biophys.* **10**, 353 (1977).
8. E. Oldfield, M. Meadows, D. Rice, R. Jacobs, *Biochemistry* **17**, 2727 (1978).
9. J. H. Davis, *Biochim. Biophys. Acta* **737**, 117 (1983).
10. M. F. Brown, *J. Chem. Phys.* **77**, 1576 (1982); ———, A. A. Ribeiro, G. R. Williams, *Proc. Natl. Acad. Sci. U.S.A.* **80**, 4325 (1983).
11. P. Meier *et al.*, *J. Phys. Chem.* **87**, 4904 (1983).
12. R. Kimmich, G. Schnur, A. Scheuermann, *Chem. Phys. Lipids* **32**, 271 (1983).
13. C. Brevard and J. P. Kintzinger, in *NMR and the Periodic Table*, R. K. Harris and B. E. Mann, Eds. (Academic Press, New York, 1978), p. 119.
14. G. Soda and T. Chiba, *J. Chem. Phys.* **50**, 439 (1969).
15. T. H. Huang, R. P. Skarjune, R. J. Wittebort, R. G. Griffin, E. Oldfield, *J. Am. Chem. Soc.* **102**, 7377 (1980).
16. D. M. Rice *et al.*, in *Proceedings of the Second SUNYA Conversation in the Discipline Biomolecular Stereodynamics*, R. H. Sarma, Ed. (Adenine, New York, 1981), vol. 2, pp. 255–270.
17. A. Blume, D. M. Rice, R. J. Wittebort, R. G. Griffin, *Biochemistry* **21**, 6220 (1982).
18. D. M. Rice *et al.*, *J. Am. Chem. Soc.* **103**, 7707 (1981).
19. R. A. Kinsey, A. Kintanar, M-D. Tsai, R. L. Smith, N. Janes, E. Oldfield, *J. Biol. Chem.* **256**, 4146 (1981).
20. M. Keniry, A. Kintanar, R. L. Smith, H. S. Gutowsky, E. Oldfield, *Biochemistry* **23**, 288 (1984).
21. D. A. Torchia and A. Szabo, *J. Magn. Reson.* **49**, 107 (1982).
22. H. W. Spiess, *J. Chem. Phys.* **72**, 6755 (1980).
23. D. Chapman, R. M. Williams, B. D. Ladbrooke, *Chem. Phys. Lipids* **1**, 445 (1967).
24. J. Seelig and A. Seelig, *Q. Rev. Biophys.* **13**, 19 (1980).
25. R. E. Jacobs and E. Oldfield, *Prog. Nucl. Magn. Reson. Spectrosc.* **14**, 113 (1981).
26. R. G. Griffin, *Methods Enzymol.* **72**, 108 (1981).
27. J. Seelig and J. L. Browning, *FEBS Lett.* **92**, 41 (1978).
28. R. Skarjune and E. Oldfield, *Biochim. Biophys. Acta* **556**, 208 (1979).
29. G. Büldt, H.-U. Gally, J. Seelig, G. Zaccai, *J. Mol. Biol.* **134**, 673 (1979).
30. R. Skarjune and E. Oldfield, *Biochemistry* **21**, 3154 (1982).
31. S. Y. Kang, H. S. Gutowsky, E. Oldfield, *ibid.* **18**, 3268 (1979).
32. S. Y. Kang *et al.*, *J. Biol. Chem.* **256**, 1155 (1981).
33. H.-U. Gally, G. Pluschke, P. Overath, J. Seelig, *Biochemistry* **19**, 1638 (1980).
34. C. P. Nichol, J. H. Davis, G. Weeks, M. Bloom, *ibid.*, p. 451.
35. I. C. P. Smith, K. W. Butler, A. P. Tulloch, J. H. Davis, M. Bloom, *FEBS Lett.* **100**, 57 (1979).
36. S. Marčelja, *Biochim. Biophys. Acta* **367**, 165 (1974).
37. H. Schindler and J. Seelig, *Biochemistry* **14**, 2283 (1975).
38. M. J. Ruocco *et al.*, *ibid.* **20**, 5957 (1981).
39. S. Ketudat and R. V. Pound, *J. Chem. Phys.* **26**, 708 (1957).
40. R. Welti, D. A. Rintoul, F. Goodsaid-Zalduondo, S. Felder, D. F. Silbert, *J. Biol. Chem.* **256**, 7528 (1981).
41. B. D. Ladbrooke, R. M. Williams, D. Chapman, *Biochim. Biophys. Acta* **150**, 333 (1968).
42. S. J. Opella, J. P. Yesinowski, J. S. Waugh, *Proc. Natl. Acad. Sci. U.S.A.* **73**, 3812 (1976).
43. H.-U. Gally, A. Seelig, J. Seelig. *Hoppe-Seyler's Z. Physiol. Chem.* **357**, 1447 (1976).
44. G. W. Stockton and I. C. P. Smith, *Chem. Phys. Lipids* **17**, 251 (1976).
45. M. G. Taylor, T. Akiyama, H. Saitô, I. C. P. Smith, *ibid.* **31**, 359 (1982).
46. R. A. Haberkorn, R. G. Griffin, M. D. Meadows, E. Oldfield, *J. Am. Chem. Soc.* **99**, 7353 (1977).
47. G. W. Stockton *et al.*, *Nature (London)* **269**, 267 (1977).
48. R. Jacobs and E. Oldfield, *Biochemistry* **18**, 3280 (1979).

49. E. Oldfield and D. Chapman, *FEBS Lett.* **23**, 285 (1972).
50. R. B. Gennis and A. Jonas, *Annu. Rev. Biophys. Bioeng.* **6**, 195 (1977).
51. D. Marsh, *Trends Biochem. Sci.* **8**, 330 (1983).
52. P. C. Jost, O. H. Griffith, R. A. Capaldi, G. Vanderkooi, *Proc. Natl. Acad. Sci. U.S.A.* **70**, 480 (1973).
53. G. B. Warren, P. A. Toon, N. J. M. Birdsall, A. G. Lee, J. C. Metcalfe, *Biochemistry* **13**, 5501 (1974).
54. A.-J. Reese, E. A. Dratz, F. W. Dahlquist, M. R. Paddy, *ibid.* **20**, 6420 (1981); A. Bienvenue, M. Bloom, J. H. Davis, P. F. Devaux, *J. Biol. Chem.* **257**, 3032 (1982).
55. E. Oldfield *et al.*, *Proc. Natl. Acad. Sci. U.S.A.* **75**, 4657 (1978).
56. A. Seelig and J. Seelig, *Hoppe-Seyler's Z. Physiol. Chem.* **359**, 1747 (1978).
57. S. Y. Kang *et al.*, *Biochemistry* **18**, 3257 (1979).
58. J. Seelig, L. Tamm, L. Hymel, S. Fleischer, *ibid.* **20**, 3922 (1981).
59. M. R. Paddy, F. W. Dahlquist, J. H. Davis, M. Bloom, *ibid.*, p. 3152.
60. M. R. Paddy and F. W. Dahlquist, *Biophys. J.* **37**, 110 (1982).
61. D. M. Rice *et al.*, *Biochemistry* **18**, 5893 (1979).
62. J. Davoust, A. Bienvenue, P. Fellmann, P. F. Devaux, *Biochim. Biophys. Acta* **596**, 28 (1980).
63. P. J. Dehlinger, P. C. Jost, O. H. Griffith, *Proc. Natl. Acad. Sci. U.S.A.* **71**, 2280 (1974).
64. A. Rousselet, P. F. Devaux, K. W. Wirtz, *Biochem. Biophys. Res. Commun.* **90**, 871 (1979).
65. O. H. Griffith, J. R. Brotherus, P. C. Jost, in *Lipid-Protein Interactions*, P. C. Jost and O. H. Griffith, Eds. (Wiley-Interscience, New York, 1982), pp. 225–237.
66. P. F. Devaux, J. Davoust, A. Rousselet, *Biochem. Soc. Symp.* **46**, 207 (1981).
67. S. Y. Kang, S. Rajan, H. S. Gutowsky, E. Oldfield, unpublished results.
68. P. K. Wolber and B. S. Hudson, *Biophys. J.* **37**, 253 (1982).
69. F. Jähnig, *Proc. Natl. Acad. Sci. U.S.A.* **76**, 6361 (1979).
70. W. Stoeckenius, R. H. Lozier, R. A. Bogomolni, *Biochim. Biophys. Acta* **505**, 215 (1979).
71. F. R. N. Gurd and T. M. Rothgeb *Adv. Protein Chem.* **33**, 73 (1979).
72. H. Frauenfelder, G. A. Petsko, D. Tsernoglou, *Nature (London)* **280**, 558 (1979).
73. P. J. Artymiuk *et al.*, *ibid.*, p. 563.
74. L. W. Jelinski, C. E. Sullivan, L. S. Batchelder, D. A. Torchia, *Biophys. J.* **32**, 515 (1980).
75. L. S. Batchelder, C. E. Sullivan, L. W. Jelinski, D. A. Torchia, *Proc. Natl. Acad. Sci. U.S.A.* **79**, 386 (1982).
76. A. Kintanar, R. Smith, E. Oldfield, in preparation.
77. E. Benedetti, in *Peptides*, M. Goodman and J. Meienhofer, Eds. (Wiley, New York, 1977), pp. 257–271.
78. J. Janin, S. Wodak, M. Levitt, B. Maigret, *J. Mol. Biol.* **125**, 357 (1978).
79. C. M. Gall, J. A. DiVerdi, S. J. Opella, *J. Am. Chem. Soc.* **103**, 5039 (1981).
80. E. Oldfield, R. A. Kinsey, A. Kintanar, *Methods Enzymol.* **88**, 310 (1982).
81. S. Schramm, A. Kinsey, A. Kintanar, T. M. Rothgeb, E. Oldfield, in *Proceedings of the Second SUNYA Conversation in the Discipline Biomolecular Stereodynamics*, R. H. Sarma, Ed. (Adenine, New York, 1981), pp. 271–286.
82. M. A. Keniry, H. S. Gutowsky, E. Oldfield, *Nature (London)*, **307**, 383 (1984).
83. D. M. Engelman, A. Goldman, T. A. Steitz, *Methods Enzymol.* **88**, 81 (1982).
84. Y. A. Ovchinnikov, *FEBS Lett.* **148**, 179 (1982).
85. K.-S. Huang, R. Radhakrishnan, H. Bayley, H. G. Khorana, *J. Biol. Chem.* **257**, 13616 (1982).
86. D. M. Engelman, R. Henderson, A. D. McLauchlan, B. A. Wallace, *Proc. Natl. Acad. Sci. U.S.A.* **77**, 2023 (1980).

RESEARCH ARTICLE

The 1984 Morgan Hill, California, Earthquake

W. H. Bakun, M. M. Clark, R. S. Cockerham, W. L. Ellsworth
A. G. Lindh, W. H. Prescott, A. F. Shakal, P. Spudich

On 24 April 1984 at 21:15:18.8 UTC (coordinated universal time), a moderate-sized (*1*) earthquake occurred on the Calaveras fault to the east of San Jose, California (Fig. 1). The earthquake was felt throughout central California (*2*), with damage estimated at $7.5 million (*3*). Because of the concentrated damage near the south end of Anderson Reservoir and the town of Morgan Hill, the 24 April event has been called the Morgan Hill earthquake.

Abstract. *The Morgan Hill, California, earthquake (magnitude 6.1) of 24 April 1984 ruptured a 30-kilometer-long segment of the Calaveras fault zone to the east of San Jose. Although it was recognized in 1980 that an earthquake of magnitude 6 occurred on this segment in 1911 and that a repeat of this event might reasonably be expected, no short-term precursors were noted and so the time of the 1984 earthquake was not predicted. Unilateral rupture propagation toward the south-southeast and an energetic late source of seismic radiation located near the southeast end of the rupture zone contributed to the highly focused pattern of strong motion, including an exceptionally large horizontal acceleration of 1.29g at a site on a dam abutment near the southeast end of the rupture zone.*

The epicenter (37°19.02'N, 121° 40.89'W) of the main shock was located on the Calaveras fault zone 5 km west-southwest of Mount Hamilton and about 65 km northwest of the junction of the Calaveras and San Andreas faults. Nearly all the aftershocks were located on the 26-km-long section of the Calaveras fault zone southeast of the epicenter of the main shock, with concentrations of aftershocks near San Felipe Valley and Anderson Reservoir (Fig. 2). We use the spatial extent of the aftershocks (Figs. 1 and 2b) to define the rupture zone of the Morgan Hill earthquake, although rupture during the main shock probably did not extend over the entire length. This distribution of the aftershocks suggests that the source mechanism of the earthquake can be described by unilateral rupture propagation south-southeast from the main shock epicenter to the south end of Anderson Reservoir.

As yet, no unambiguous surface fault rupture has been found. Prominent discontinuous postearthquake surface cracks in the fault zone near the south end of Anderson Reservoir may be the result of slumping during the strong shaking rather than an expression of fault slip. No coseismic fault slip was observed at the small-aperture Grant Ranch geodetic network located in Halls Valley 5 km northwest of the main shock epicenter (*4*). The nearest creepmeter, at Shore Road (Fig. 1a), recorded 12.9 mm of surface slip in the 18 hours after the Morgan Hill earthquake (*5*).

There are, as yet, no identified precursors that might have permitted a prediction of the time of the 1984 Morgan Hill earthquake (*6*). The rupture zone lies within the dense network of seismographic stations operated by the U.S. Geological Survey in central California so that all earthquakes there with magnitude ≥ 1.5 are recorded and located. Only two foreshocks, both magnitude <1.0, were observed (*7*). Significant activity did occur near the two ends of the rupture zone in the 16 months before the Morgan Hill earthquake (Fig. 2c); the pattern of precursory seismicity near the ends of the rupture is consistent with seismicity observed before large earthquakes on plate boundaries (*8*) and also

W. H. Bakun, M. M. Clark, R. S. Cockerham, W. L. Ellsworth, A. G. Lindh, W. H. Prescott, and P. Spudich are with the U.S. Geological Survey, Menlo Park, California 94025. A. F. Shakal is with the California Division of Mines and Geology, Sacramento 95814.